THE JOURNAL OF BIOLOGICAL CHEMISTRY VOL. 284, NO. 13, pp. 8439–8448, March 27, 2009

Synaptic Vesicle Protein NTT4/XT1 (SLC6A17) Catalyzes Na^+-coupled Neutral Amino Acid Transport*

Received for publication, August 19, 2008, and in revised form, January 15, 2009 Published, JBC Papers in Press, January 15, 2009, DOI 10.1074/jbc.M806407200

Kimberly A. Zaia and Richard J. Reimer[1]

From the Department of Neurology and Neurological Sciences and Neuroscience Graduate Program, Stanford University, Stanford, California 94305

The SLC6 family of structurally related, Na^+-dependent transporter proteins is responsible for presynaptic reuptake of the majority of neurotransmitters. Within this family are a number of orphan transporters, including NTT4/XT1 (SLC6A17), a protein first identified over 15 years ago. NTT4/XT1 is expressed exclusively in the nervous system and specifically on synaptic vesicles in glutamatergic and some GABAergic neurons. Despite extensive efforts by a number of groups, no substrate has been reported for NTT4/XT1. Here we use a combination of molecular manipulations to increase expression of the NTT4/XT1 protein at the plasma membrane and to directly demonstrate that it catalyzes neutral amino acid transport. The substrate profile of the NTT4/XT1-dependent activity is similar to that of the closely related B^0AT2/SBAT1 (SLC6A15), including a submillimolar apparent affinity for proline and leucine and a low millimolar apparent affinity for glutamine. The transport activity is Na^+-dependent and Cl^--independent and is inhibited by low pH as is SLC6A15, suggesting redundant roles for these proteins. This characterization of NTT4/XT1 offers important insights into neurotransmitter metabolism as well as the mechanistic differences among the structurally related, but functionally divergent, SLC6 proteins.

Synaptic transmission places a great metabolic burden upon neurons. The thousands of neurotransmitter molecules released with fusion of each synaptic vesicle must be replenished. The most direct mechanism of compensating for exocytotic release is presynaptic reuptake of the neurotransmitter through plasma membrane transporters. Such a reuptake mechanism is used by several types of neurons, including those that release GABA,[2] glycine, and monoamines. The fates of synaptically released acetylcholine and glutamate are more complex; acetylcholine is hydrolyzed to acetate and choline in the synaptic cleft, and synaptically released glutamate is readily taken up by astrocytes, precluding direct neuronal reuptake of these neurotransmitters. Although acetylcholine is hydrolyzed in the synaptic cleft, a presynaptic transport system for the choline portion of the neurotransmitter is expressed in cholinergic neurons (1). Glutamate cleared from the synapse by astrocytes is rapidly converted to glutamine and shuttled back into neurons for reconversion to glutamate (2). Despite the efficiency of astrocytic glutamate uptake, it is estimated that at least 25% of the synaptically released glutamate exits this glutamate-glutamine cycle (3), suggesting that glutamatergic neurons must rely on additional transport mechanisms for uptake of neurotransmitter precursors.

The SLC6 family, a group of structurally related, Na^+-dependent transporter proteins, is responsible for presynaptic reuptake of the majority of neurotransmitters (4, 5). These transporters can be subdivided into the following groups on the basis of structure: 1) a monoamine transporter group (DAT, NET, and SERT); 2) a GABA transporter group that includes GAT1–3 as well as betaine, taurine, and creatine transporters; 3) an amino acid transporter group consisting of the glycine transporters GlyT1 and GlyT2, the proline transporter PROT, and the neutral and cationic amino acid transporter ATB(0+); and 4) a second amino acid transporter group consisting of two imino transporters (one expressed in kidney and one in brain), the two broad specificity neutral amino acid transporters B^0AT1 and B^0AT2/SBAT1, and a number of orphan transporters.

Included in the group of orphan transporters is NTT4/XT1 (SLC6A17), a protein first identified over 15 years ago in a screen for sequences related to the GABA and monamine transporters (6, 7) The exclusive expression of SLC6A17 in the nervous system and the close sequence relationship to the known neurotransmitter transporters (NTTs) led to its designation as NTT4. Although NTT4/XT1 is expressed only in glutamatergic and some GABAergic neurons, no substrate has been reported despite extensive efforts by a number of groups (5–7). The challenge in delineating substrate specificity for NTT4/XT1 has been attributed to the likelihood that the protein, which is present on synaptic vesicles *in vivo*, is not trafficked to the plasma membrane when heterologously expressed (5). The recent demonstration that SLC6A15 (B^0AT2/SBAT1), the protein most closely related to NTT4/XT1, is a neutral amino acid transporter (8, 9) has led to the suggestion that NTT4/XT1 is also a neutral amino acid transporter (5). Here, we test this hypothesis by modifying NTT4/XT1 to increase surface expression of the recombinant protein in transfected

* This work was supported, in whole or in part, by National Institutes of Health Grant K02 NS045634. This work was also supported by a National Defense Science and Engineering Graduate fellowship (to K. A. Z.) and a grant from The Dana Foundation Brain and Immuno-Imaging (to R. J. R.). The costs of publication of this article were defrayed in part by the payment of page charges. This article must therefore be hereby marked "*advertisement*" in accordance with 18 U.S.C. Section 1734 solely to indicate this fact.

[1] To whom correspondence should be addressed: P211 MSLS, 1201 Welch Rd., Stanford, CA 94305. Fax: 650-498-6262; E-mail: rjreimer@stanford.edu.

[2] The abbreviations used are: GABA, γ-aminobutyric acid; TM, transmembrane; HA, hemagglutinin antigen; DMEM, Dulbecco's modified Eagle's medium; PBS, phosphate-buffered saline; MOPS, 4-morpholinepropanesulfonic acid; PNS, post-nuclear supernatant; NTT, neurotransmitter transporter; NaGluc, sodium gluconate; SERT, serotonin transporter; NMDG, *N*-methyl-D-glucamine.

HEK293T cells. Using this system we directly demonstrate that NTT4/XT1 is a neutral amino acid transporter with a substrate profile similar to B^0AT2/SBAT1, including a submillimolar apparent affinity for proline and leucine and a low millimolar apparent affinity for glutamine. The transport activity is Na^+-dependent and Cl^--independent and is inhibited by low pH as is SLC6A15, suggesting a potential redundancy of function for these proteins. We also express wild-type NTT4/XT1 in PC12 cells and demonstrate a coupling of vesicle exocytosis with increased amino acid uptake. This finding suggests that in the setting of neuronal activity the vesicular localization of NTT4/XT1 *in vivo* facilitates redistribution of the transporter to the plasma membrane where it functions as a Na^+-dependent neutral amino acid transporter.

EXPERIMENTAL PROCEDURES

Cloning—The coding sequences for the rat isoforms of SLC6A15 (B^0AT2/SBAT1) and SLC6A17 (NTT4/XT1) were amplified from rat brain cDNA and initially subcloned into the pCR-2.1-TOPO vector (Invitrogen). Carboxyl-terminal tagged full-length NTT4/XT1 constructs (NTT4/XT1-wt) were generated by first amplifying the coding sequence with primers containing 5′ HindIII and 3′ NotI restriction site sequences and subcloning the resultant PCR product into a pcDNA3 vector (Invitrogen) as modified below. Carboxyl-terminal tagged chimeric NTT4/XT1 constructs (NTT4/XT1-chi) were generated by amplifying the coding sequences for amino acids 1–653 of the rat NTT4/XT1 and the predicted cytosolic carboxyl-terminal domain of the rat B^0AT2 (amino acids 656–729) with primers engineered to include 5′ HindIII and 3′ ClaI sites and 5′ ClaI and 3′ NotI sites, respectively. The amino-terminal NTT4/XT1 PCR product was subcloned in-frame with the carboxyl-terminal B^0AT2/SBAT1 PCR product in pcDNA3, resulting in the following bridging sequence NTLSV**ID**TYKRG. The isoleucine and aspartate (indicated in boldface type) separate the NTT4/XT1 and B^0AT2/SBAT1 fragments.

For tagging of carboxyl termini, a hemagglutinin antigen (HA) tag (YPYDVPDYA) followed by a stop codon or the enhanced green fluorescent protein coding sequence followed by a stop codon was subcloned downstream of, and in-frame with, NTT4/XT1-wt or NTT4/XT1-chi coding sequences in pcDNA3 using 5′ NotI and 3′ XbaI restriction sites. The sequences of all PCR products were confirmed by a commercial facility (Biotech Core Inc., Sunnyvale, CA).

Cell Culture and Transfection—Human embryonic kidney 293T (HEK293T) cells were maintained in Dulbecco's modified Eagle's medium (DMEM; Invitrogen) supplemented with 10% cosmic calf serum (HyClone, Logan, UT) and 1% penicillin/streptomycin (Sigma) at 37 °C in 5% CO_2. Two days before each assay, 24-well Nunc culture plates (Thermo Fisher Scientific, Rochester, NY) were incubated for at least 1 h with a poly-D-lysine hydrobromide solution (Invitrogen) followed by an additional 1-h incubation in a 1:100 solution of Matrigel (BD Biosciences) in DMEM. Each well was then plated with ~90,000 HEK293T cells in a final volume of 500 μl of media. The following day, cells were transfected by the calcium phosphate method (10) with 0.75 μg of DNA per well. Unless otherwise indicated, a combination of 0.5 μg of NTT4/XT1-chi plasmid DNA and 0.25 μg of dynamin K44A plasmid DNA (11) was used. For control cells, 0.5 μg of plasmid DNA encoding a nonfunctioning H183R mutant of the lysosomal sialic acid transporter sialin (12) was used to replace the NTT4/XT1-chi plasmid DNA. Cell counts per well at the time of the assay were 252,000 ± 9800 control-transfected cells and 240,500 ± 7000 NTT4/XT1-chi-transfected cells, indicating no significant difference in cell viability ($p < 0.4$).

PC12 cells were maintained in DMEM supplemented with 10% horse serum, 5% cosmic calf serum, and 1% penicillin/streptomycin. Serum deprivation (DMEM with 1% horse serum and 1% penicillin/streptomycin) in the presence of nerve growth factor (50 ng/ml) for 4 days was used to differentiate PC12 cells. To generate PC12 cells stably expressing NTT4/XT1, wild-type PC12 cells were transfected with pcDNA3 vector containing the HA-tagged wild-type NTT4/XT1 sequence using Lipofectamine 2000 (Invitrogen) following the protocol of the manufacturer. Clonal cell lines with the plasmid stably integrated were selected for by resistance to G418 (0.5 mg/ml, Invitrogen). Immunofluorescence staining (see below) was used to identify lines expressing high levels of the recombinant protein.

Fluorescence Imaging—Cells were plated on coverslips pretreated with poly-D-lysine hydrobromide and Matrigel. HEK293T cells were transfected as described above and ~24 h post-transfection fixed with 4% paraformaldehyde in PBS for 20 min at 4 °C. PC12 cells were similarly plated and fixed. The HA-tagged proteins in transfected HEK293T cells were immunostained, as described previously (12), with a monoclonal mouse α-HA primary antibody (Covance, Princeton, NJ) at 1:2000 and goat α-mouse fluorescently labeled (Alexa 488) secondary antibody (Molecular Probes, Invitrogen) at 1:1000. For double-labeling studies the stably transfected PC12 cells were plated similarly but differentiated as described above. Cells were immunostained with rabbit α-HA (AbCAM) and mouse α-synaptobrevin (Synaptic Systems) primary antibodies diluted at 1:1000 and 1:3000, respectively, and fluorescently labeled donkey α-rabbit rhodamine Red-X (Jackson ImmunoResearch) and goat α-mouse Alexa 488 (Molecular Probes) secondary antibodies at 1:1000. Fluorescence images were collected with a Zeiss Axiovert microscope using Openlab 3.5.1 software (Improvision Inc., Waltham, MA).

Protease Protection Assay—HEK293T cells were plated, and each well was transfected with 0.5 μg of plasmid DNA encoding wild-type NTT4/XT1-HA or the carboxyl-terminal chimeric NTT4/XT1-HA as described above. Approximately 22 h post-transfection, cells were rinsed twice in PBS containing 1 mM $CaCl_2$ and 0.5 mM $MgCl_2$, rinsed once in Ca^{2+}/Mg^{2+}-free PBS, resuspended in 600 μl of Ca^{2+}/Mg^{2+}-free PBS, and transferred to an Eppendorf tube. Trypsin (Invitrogen) was added directly to the suspended cells at a final concentration of 0.1 μg/μl. The reaction was terminated immediately ($t = 0$) or after 10 min at room temperature ($t = 10$) by the transfer of 100-μl aliquots of the trypsin/cell suspension to separate tubes containing 12 μl of soybean trypsin inhibitor (5 μg/μl, USB Corp., Cleveland, OH) for a final concentration of 0.54 μg/μl. Samples were separated on a reducing SDS-polyacrylamide gel, transferred to polyvinylidene difluoride membranes (Pall), and immunoblotted with

a mouse monoclonal α-HA primary antibody (Covance) and a rabbit α-mouse IgG-horseradish peroxidase secondary antibody (Pierce) as described previously (12). Detection of hybridization was done with chemiluminescence (Amersham Biosciences) and exposure of the blot to autoradiography film (Cole Parmer Blue-Sensitive) for 15 s to 5 min. The resulting signal was quantified with ImageJ, and the fraction of protein per well sensitive to trypsin cleavage was calculated as the fractional reduction in signal intensity between $t = 0$ and $t = 10$.

Transport Assay—Uptake measurements were made 22–24 h following transfection for transiently transfected cells or 18–20 h after plating stably transfected PC12 cells (350,000 cells/well in a 24-well plate). Briefly, cell culture media were removed from each well by vacuum aspiration and replaced with 1 ml of assay buffer containing 4.7 mM KCl, 1.2 mM $MgSO_4$, 2.2 mM $CaCl_2$, 0.4 mM KH_2PO_4, 10 mM D(+)-glucose, 10 mM HEPES, MOPS, or Tris buffer and 120 mM NaCl, sodium gluconate (NaGluc) or the indicated salt. For PC12 cells, Krebs-Ringers/HEPES (120 mM NaCl, 4.7 mM KCl, 1.2 mM $MgSO_4$, 0.4 mM KH_2PO_4, 10 mM D(+)-glucose, and 10 mM HEPES, pH 7.4) with no $CaCl_2$ or 2.2 mM $CaCl_2$ was used as the assay buffer. After incubation in assay buffer of the specified pH and salt composition for 5 min at 37 °C, the buffer was removed by aspiration and replaced with 250 μl of reaction buffer consisting of assay buffer plus 0.5 μCi of the radioactive amino acid ([^{3}H]Pro or [^{3}H]Gln; American Radiolabeled Chemicals, Inc., St. Louis) to yield final concentrations of 0.02 and 0.04 pmol/μl for Pro and Gln, respectively. Additional reagents (*i.e.* valinomycin, ionomycin, potassium tartrate, ammonium tartrate, or unlabeled substrate) were added to the reaction buffer as specified. Cells were incubated in reaction buffer at 37 °C for the indicated times, and the reaction was terminated by addition of 1 ml of ice-cold assay buffer followed by two additional washes in 1 ml of ice-cold assay buffer. After removal of the final wash, cells were solubilized in 250 μl of 1% SDS, and [^{3}H] amino acid content was determined by liquid scintillation counting. To measure background for experiments using transiently transfected HEK293T cells, control cells were transfected with a previously characterized plasma membrane-targeted nonfunctioning H183R mutant of the lysosomal sialic acid transporter sialin (12). Uptake in wild-type PC12 cells was assayed as background for experiments with stably transfected PC12 cells. For vesicular transport assays, post-nuclear supernatants (PNS) were prepared by resuspending pelleted PC12 cells in 0.3 M sucrose, 10 mM HEPES-KOH, pH 7.4 (SH buffer), containing protease inhibitors (in μg/ml: 2 aprotinin, 1 leupeptin, 2 antipain, 10 benzamidine, 35 phenylmethanesulfonyl fluoride, 1 chymostatin, 1 pepstatin,) along with 1.25 mM MgEGTA. The cells were disrupted by homogenization at 4 °C through a ball-bearing cell homogenizer with a 10-μm clearance, and nuclear debris was sedimented at 1000 × *g* for 5 min to yield the PNS. 200 μg of PNS in 50 μl was added to 200 μl of uptake buffer (100 mM NaCl, 20 mM HEPES, 2.5 mM $MgSO_4$, 2 mM ATP, pH 7.4) with 22 nM of [^{3}H]Pro and incubated for 6–10 min. The reaction was terminated by rapid filtration through polyethersulfone membranes (Supor 200, Pall), followed by immediate washing two times with 1.5 ml of cold uptake buffer. The bound radioactivity was measured by scintillation counting in 3 ml of Cytoscint (ICN). Background was subtracted for all analyses.

Calculations—Uptake of radioactive amino acids was independently measured in duplicate wells of control and NTT4/XT1-transfected cells for each condition in a minimum of three separate independent experiments. Scintillation counts were converted into molar quantities by calibration of a given volume of [^{3}H]Pro or [^{3}H]Gln with specific activity data provided by the manufacturer (ARC, Inc.). Specific NTT4/XT1-mediated amino acid uptake was calculated as the difference in uptake between control-transfected wells and NTT4/XT1-transfected wells assayed under parallel experimental conditions. For the protease protection assay, samples from three independent experiments were analyzed. Error bars represent the means ± S.E. of the average values from independent experiments. Statistical significance is indicated by single ($p < 0.05$) or double ($p < 0.01$) asterisks. All linear and nonlinear regression analyses were performed in Prism5 (GraphPad Software Inc., La Jolla, CA). The concentration of unlabeled substrate that inhibits specific NTT4/XT1-mediated [^{3}H]Pro uptake by 50% (IC_{50}) was calculated from the linear regression of normalized uptake *versus* the logarithm of the concentration of unlabeled substrate. The K_m and V_{max} values for Pro and Gln were calculated from the nonlinear regression of specific NTT4/XT1-mediated amino acid uptake velocity *versus* the extracellular concentration of Pro and Gln, respectively.

RESULTS

Sequence Comparisons Predict that NTT4/XT1 Mediates Na^+-dependent, Cl^--independent Proline Transport—The SLC6 family is a group of structurally related proteins that transport amino acids and other small organic molecules. The recent determination of the tertiary structure of the related bacterial amino acid transporter LeuT has led to the identification of specific residues and regions that are involved in binding of substrate and transported ions (13). An alignment of NTT4/XT1 with its most closely related family member, B^0AT2/SBAT1, indicates a high degree of sequence similarity between the two proteins (66% identity) with the greatest divergence in the last transmembrane region and the cytosolic amino and carboxyl termini (Fig. 1). There is an absolute conservation of residues in B^0AT2/SBAT1 and NTT4/XT1 in the positions implicated in binding the substrate and sodium ions. A comparison with the structurally related human SERT indicates that of the four residues implicated in binding a Cl^- ion (14, 15), the residues corresponding to Tyr-121, Asn-368, and Ser-372 in SERT are conserved in B^0AT2/SBAT1 and NTT4/XT1, whereas the residue corresponding to Ser-336 in SERT is an alanine in B^0AT2/SBAT1 and NTT4/XT1. The absolute conservation of the ion- and substrate-binding residues in B^0AT2/SBAT1 and NTT4/XT1 suggests that these proteins transport similar substrates with similar ionic dependence. This predicts that NTT4/XT1 is a Na^+-dependent, Cl^--independent neutral amino acid transporter, but previous attempts at measuring such activity have been unsuccessful (5–7).

Cytosolic Carboxyl Terminus of NTT4/XT1 Influences Targeting to Intracellular Vesicles—Previous work has revealed

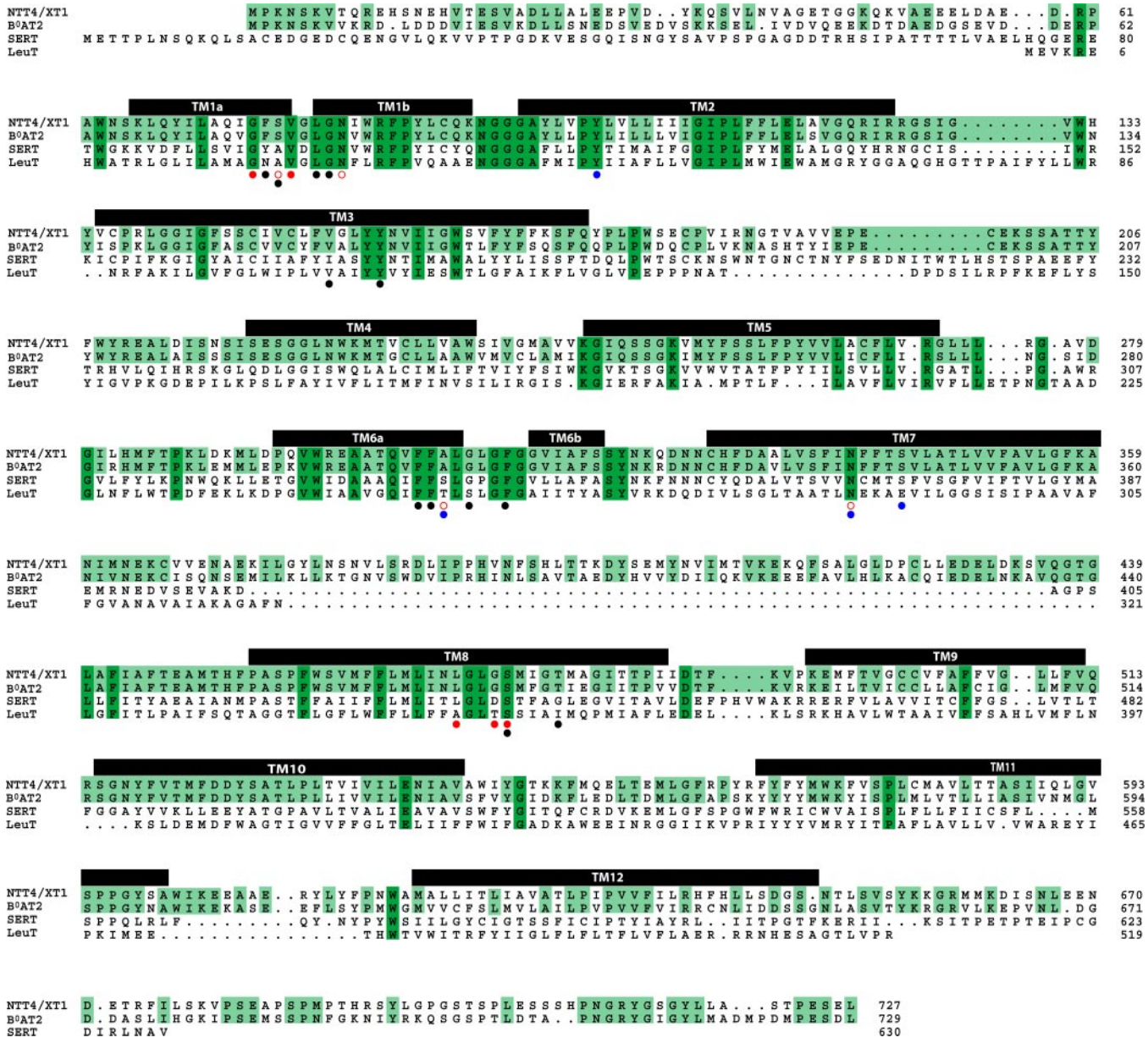

FIGURE 1. **Comparison of NTT4/XT1 and B^{0}AT2/SBAT1 sequences suggests similar biochemical functions.** The predicted amino acid sequences of rat NTT4/XT1 and B^{0}AT2/SBAT1 along with human SERT serotonin transporter and *Aquifex aeolicus* LeuT are aligned using the Pileup program (GCG version 11.1.2) with manual adjustments. *Dark green shaded boxes* indicate residues strictly conserved across all four proteins, and *light green boxes* indicate additional residues that are identical in the NTT4/XT1 and B^{0}AT2/SBAT1 sequences. Transmembrane domains (*TM1–12*) are indicated by *black bars above* the corresponding residues. The *open* and *filled red circles* show residues involved in coordinating sodium ions Na_1 and Na_2, respectively, whereas the *black circles* indicate residues involved in substrate binding by LeuT according to Yamashita *et al.* (13). The *blue circles* denote residues involved in Cl^- binding by SERT according to Forrest *et al.* (14). There is a high overall degree of similarity between NTT4/XT1 and B^{0}AT2/SBAT1 (66% identity) and an absolute conservation between the proteins for the residues involved in substrate and ion binding.

that NTT4/XT1 is localized to synaptic vesicles *in vivo* (16). We anticipated that targeting NTT4/XT1 to the plasma membrane could facilitate a functional analysis of the transporter. For B^{0}AT2/SBAT1, studies on the localization of the heterologously expressed protein (17) suggest that the protein resides on the plasma membrane, a conclusion that is supported by the recent demonstration of transport activity in *Xenopus* oocytes (8, 9). Because trafficking motifs for membrane proteins are typically present in cytosolic domains, we looked for cytosolic regions of NTT4/XT1 and B^{0}AT2/SBAT1 with greatest sequence variation to identify sequences that might target NTT4/XT1 to intracellular membranes. Of the predicted cytosolic domains, the carboxyl terminus exhibits the greatest divergence (42% identity). To determine whether the carboxyl terminus contributes to the different subcellular localization of NTT4/XT1 and B^{0}AT2/SBAT1, we generated a chimeric protein in which the carboxyl terminus of NTT4/XT1 is replaced with the corresponding region of B^{0}AT2/SBAT1. Immunofluorescence studies demonstrate that the wild-type NTT4/XT1 protein is targeted to intracellular membranes when heterologously expressed in HEK293T cells (Fig. 2*A*, *left panel*). In comparison, the immunostaining pattern of the chimeric NTT4/XT1 protein suggests a pool of protein on intracellu-

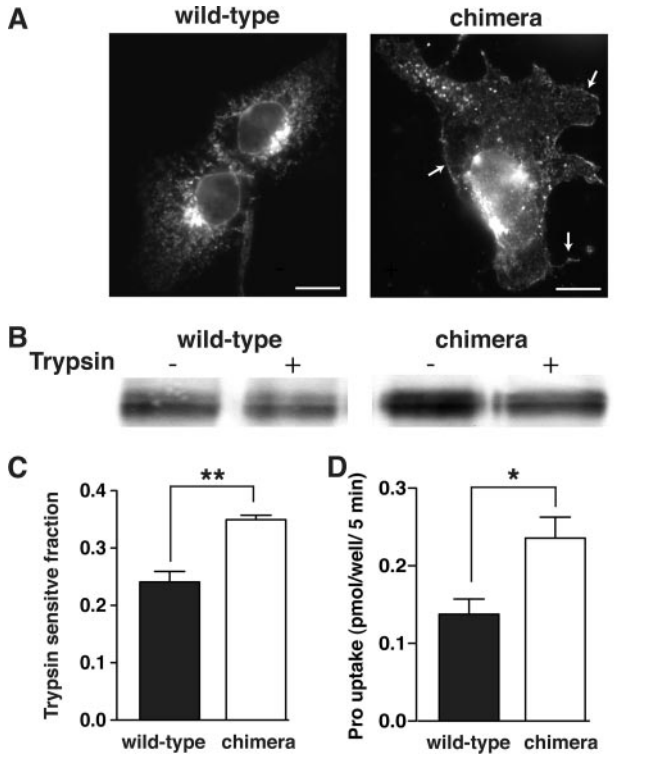

FIGURE 2. **NTT4/XT1 chimeric protein exhibits enhanced plasma membrane expression and transport activity in HEK293T cells.** *A,* heterologously expressed wild-type (*left*) and chimeric (*right*) NTT4/XT1 proteins were visualized in transfected HEK293T cells by fluorescence microscopy (*scale bar,* 10 μm). The wild-type protein predominantly localizes to an intracellular population of vesicles. Expression of the chimeric NTT4/XT1 protein in which the carboxyl terminus has been replaced with that of B^0AT2/SBAT1 enhances staining of the plasma membrane (*arrows*). *B,* immunoblotting of cell extracts with α-HA antibodies shows the relative amount of full-length heterologously expressed wild-type (*left*) and chimeric (*right*) NTT4/XT1 proteins before (−) and after (+) 10 min of exposure of suspended cells to trypsin. *C,* trypsin-sensitive fraction of wild-type and chimeric proteins was quantified as the fractional decrease in the intensity of immunoblotted signal corresponding to the presence of full-length heterologously expressed protein. The trypsin-sensitive fraction is 1.5-fold greater in cells expressing the chimeric protein (** indicates $p < 0.01$). *D,* Pro uptake (pmol of Pro/well/5 min) was quantified in HEK293T cells transfected with 0.5 μg of control (*i.e.* nonfunctional sialin), NTT4/XT-wt, or NTT4/XT1-chi plasmid DNA after a 5-min incubation of cells in assay buffer (120 mM NaGluc, pH 8.5, ** indicates $p < 0.01$). *E,* specific NTT4/XT1-mediated Pro uptake (pmol/well/5 min) was quantified by subtracting uptake in cells transfected with control DNA from uptake in cells expressing NTT4/XT1-wt or NTT4/XT1-chi (* indicates $p < 0.05$).

lar vesicles but a greater degree of plasma membrane targeting (Fig. 2*A*, *right panel*).

To confirm this finding we used a protease protection assay to assess the relative amount of protein on the cell surface. We specifically examined the sensitivity of the heterologously expressed wild-type and chimeric NTT4/XT1 proteins to trypsinization in intact cells. Because NTT4/XT1 has several trypsin cleavage sites in predicted extracellular loops, protein on the cell surface should be digested by trypsin, whereas protein localized to intracellular vesicles should be insensitive to the exogenous protease. Quantification of Western blot signals of extracts from cells expressing the HA-tagged proteins (Fig. 2*C*) indicate that incubation with trypsin results in a loss of 24 ± 2% of the wild-type protein and 35 ± 1% of the chimeric protein. This finding suggests a higher level of plasma membrane expression when the carboxyl terminus of NTT4/XT1 is replaced with that of B^0AT2/SBAT1 and is consistent with our immunofluorescence data. Whereas these data indicate that the carboxyl terminus of NTT4/XT1 has some role in trafficking, the presence of a large intracellular pool of chimeric protein suggests that other domains in NTT4/XT1 likely contribute to vesicular targeting of the protein.

Because recent studies have demonstrated that B^0AT2/SBAT1 mediates pH-sensitive proline transport with a submillimolar apparent affinity (8, 9), we hypothesized that NTT4/XT1 would have similar transport activity and that increased expression of the chimeric protein on the cell surface would correlate with increased uptake. Indeed uptake of radiolabeled proline in pH 8.5 buffer was 2.4- and 3.4-fold greater in HEK293T cells expressing wild-type and chimeric NTT4/XT1, respectively, as compared with control cells (Fig. 2*D*). Furthermore, specific NTT4/XT1-mediated proline uptake (as calculated by subtracting uptake in control cells from uptake in NTT4/XT1-expressing cells) was 1.7-fold greater in cells expressing the chimeric protein than in cells expressing the wild-type protein (Fig. 2*E*, $p < 0.02$).

NTT4/XT1 Mediates Na^+-dependent, Cl^--independent Proline Transport—Because much of the chimeric protein is intracellular, we sought to increase the amount of protein at the plasma membrane in an attempt to increase measurable NTT4/XT1-mediated proline uptake even further. To do so, we co-expressed chimeric NTT4/XT1 (NTT4/XT1-chi) with a dominant negative isoform of dynamin (dynamin K44A), which has been shown to decrease endocytosis of proteins from the plasma membrane (1, 11). Cells co-transfected with dynamin K44A exhibited 3-fold greater proline uptake than control cells at both pH 7.4 and pH 8.5 (Fig. 3*A*). Although background is increased (compare Fig. 3, *A, pH 8.5 control,* to *D*, control), this co-expression approach enhances specific NTT4-XT1-mediated uptake activity at pH 8.5 by 34% ($p < 0.02$; Fig. 2*D* and Fig. 3*A*).

To assess ionic dependence of NTT4/XT1-mediated proline transport, we next compared uptake of radiolabeled proline in assay buffer containing NaCl, NaGluc (Cl^--free), and NMDG-tartrate (Na^+- and Cl^--free). Specific NTT4/XT1-mediated uptake is not significantly different in NaCl *versus* NaGluc, suggesting Cl^- independence; however, uptake is strongly inhibited in NMDG-tartrate as compared with NaCl or NaGluc, demonstrating Na^+ dependence (Fig. 3*B*). Uptake in assay buffer containing sodium tartrate is comparable with uptake in NaCl and NaGluc (data not shown). These results indicate that, similar to B^0AT2/SBAT1, NTT4/XT1 catalyzes proline transport in a Na^+-dependent, Cl^--independent fashion.

To examine the time dependence of proline uptake, NTT4/XT1-chi and control-transfected HEK293T cells were incubated with radiolabeled proline in assay buffer containing NaGluc, pH 8.5, for 0–60 min (Fig. 3*C*). Proline uptake was greater in NTT4/XT1-chi-transfected cells at all time points. A subtraction of the endogenous proline uptake from the uptake observed with NTT4/XT1-chi (Fig. 3*D*) shows that specific NTT4/XT1-chi-mediated proline uptake reaches a steady state within ~20 min.

To further examine sodium dependence of specific NTT4/XT1-chi-mediated uptake in transfected HEK293T cells, we

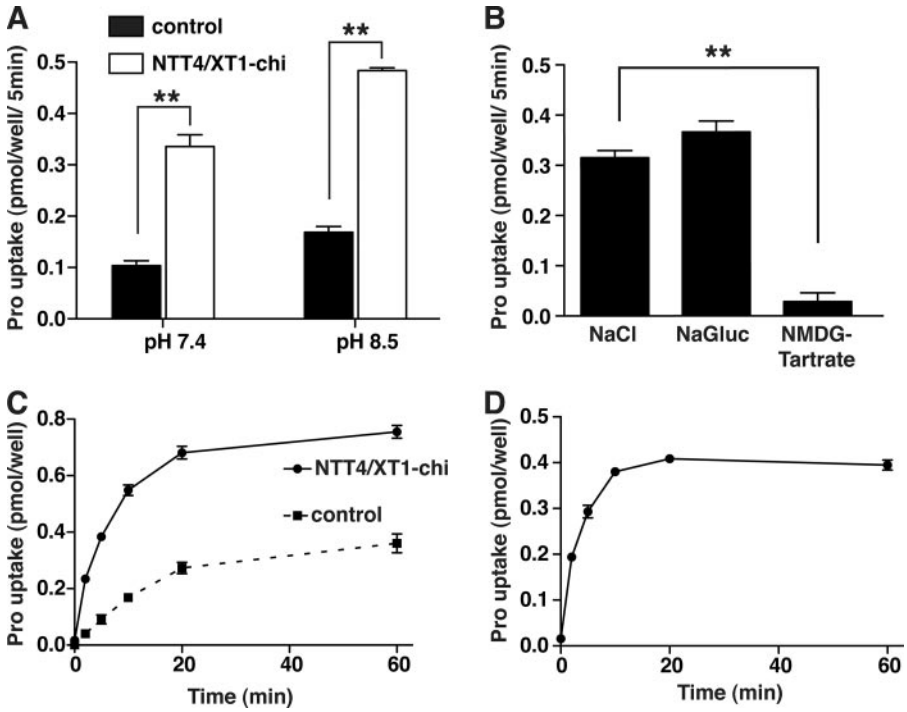

FIGURE 3. **NTT4/XT1 mediates Na^+-dependent, Cl^--independent Pro uptake in transfected HEK293T cells.** *A,* Pro uptake was quantified in HEK293T cells co-transfected with 0.25 μg of dynamin K44A plasmid DNA and either 0.5 μg of NTT4/XT1-chi or control (*i.e.* nonfunctional sialin) plasmid DNA. Analysis of Pro uptake (plotted as pmol/well/5 min) during a 5-min incubation in assay buffer (120 mM NaGluc) demonstrates a 3.2- and 2.9-fold increase over background at pH 7.4 and pH 8.5, respectively. *B,* Pro uptake into transfected HEK293T cells was quantified after a 5-min incubation of cells in assay buffer, pH 8.5, containing either 120 mM NaCl (*left*), 120 mM NaGluc (*center*), or 120 mM NMDG-tartrate (*right*), demonstrating Cl^- independence and Na^+ dependence of transport. NTT4/XT1-chi-mediated Pro uptake was obtained by subtracting uptake in cells transfected with control DNA from uptake in cells transfected with NTT4/XT1-chi DNA. *C,* time course of Pro uptake into HEK293T cells transfected with NTT4/XT1-chi or control DNA after incubation of cells in assay buffer (120 mM NaGluc, pH 8.5) for various lengths of time demonstrates greater uptake in the NTT4/XT1-chi-transfected cells at all time points. Plotted data are from duplicate samples of a representative experiment. *D,* NTT4/XT1-chi-mediated proline uptake was determined by subtracting uptake in control cells from uptake in NTT4/XT1-chi-expressing cells. Uptake is saturated by 20 min. *Asterisks* in *A* and *B* indicate statistical significance ($p < 0.01$).

quantified uptake of radiolabeled proline in assay buffer containing 0–120 mM sodium, pH 8.5, for 5 min at 37 °C. Equimolar ionic concentrations were maintained by combining sodium tartrate with NMDG and tartaric acid to achieve the desired [Na^+]. The specific NTT4/XT1-chi-mediated proline uptake shows a hyperbolic dependence on extracellular sodium (Fig. 4*A*) with a nonlinear regression using a least squares (ordinary) fit of the data indicating a half-maximal uptake at [Na^+] = 23 mM.

NTT4/XT1-chi-mediated Proline Transport Is Dependent on Membrane Potential and pH—Given that B^0AT2/SBAT1 transport is electrogenic (8, 9), we next examined the dependence of proline uptake by NTT4/XT1-chi on membrane potential (Fig. 4*B*). Uptake was reduced by 12% with the addition of 20 μM of the potassium ionophore valinomycin (val), 55% with the addition of 25 mM potassium tartrate (K^+), and 63% with the addition of both valinomycin and potassium tartrate. Because increasing extracellular potassium ions depolarizes the membrane and valinomycin enhances this effect, the resulting reduction in NTT4/XT1-chi-mediated proline uptake is consistent with an electrogenic transport mechanism.

B^0AT2/SBAT1 and other members of the SLC6 family mediate pH-dependent transport (9, 18, 19); thus we next sought to determine whether the activity of NTT4/XT1 is also modulated by pH. To test pH dependence, we measured specific NTT4/XT1-chi-mediated proline uptake in buffer solutions of different pH. Similar to B^0AT2/SBAT1, NTT4/XT1-chi-mediated proline transport is inhibited by low pH with little measurable transport at pH 5.5 (Fig. 4*C*). Uptake increases linearly with increasing pH from pH 6.5 to 8.0. The pH sensitivity could be the result of the coupled counter-transport of H^+ or changes in the protonation state of an extracellular residue(s) that alter substrate binding or transport. To determine whether the transmembrane pH gradient (ΔpH) could be contributing to the driving force for proline uptake, we used ammonium ions to dissipate the gradient. At pH 8.5, a condition in which the extracellular pH is higher than the intracellular pH, addition of 10 mM ammonium tartrate significantly reduces proline uptake; however, at pH 7.2 where ΔpH is very small, addition of ammonium tartrate does not affect uptake (Fig. 4*D*). These data suggest that ΔpH contributes to the driving force for proline transport by coupling H^+ antiport to proline uptake. However, at pH 6.5 the inhibitory effect of low pH is not reversed by the addition of ammonium tartrate.

NTT4/XT1-chi-mediated Proline Transport Is Inhibited by Neutral Amino Acids—Given that members of the SLC6 family have been shown to transport a variety of different amino acids (4, 5), we next examined substrate specificity of NTT4/XT1-chi using an inhibition assay. We measured the uptake of radiolabeled proline in the absence and presence of 5 mM unlabeled amino acids (Fig. 5*A*). As normalized to [^{3}H]proline uptake in the absence of unlabeled amino acids, uptake is most efficiently inhibited by neutral amino acids. Specific NTT4/XT1-chi-mediated proline uptake is reduced by at least 90% in the presence of leucine, methionine, or proline, at least 75% in the presence of cysteine, alanine, glutamine, or serine, and at least 50% in the presence of histidine or glycine. Proline uptake is also significantly inhibited by the amino acids α-methylaminoisobutyric acid, D-serine, α-aminoisobutyric acid, and glutamate, although to a much lesser degree. Pyroglutamic acid, GABA, and arginine have no effect on uptake.

To further characterize and compare the inhibition of [^{3}H]Pro uptake by leucine, proline, and glutamine, we measured uptake of [^{3}H]Pro in the presence of 0–10 mM unlabeled substrate. As analyzed with a linear regression of normalized

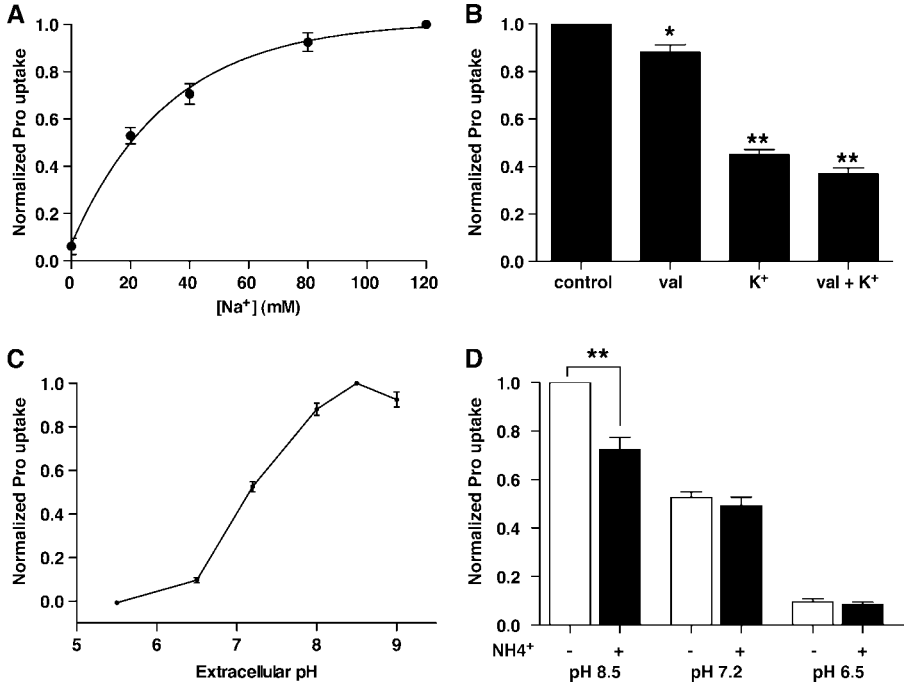

FIGURE 4. **NTT4/XT1-mediated Pro uptake is dependent on extracellular [Na^+], membrane potential, and pH.** *A,* NTT4/XT1-chi-mediated Pro uptake quantified after a 5-min incubation of transfected HEK293T cells in assay buffer, pH 8.5, containing varying concentrations of Na^+ tartrate with ionic substitution of NMDG-tartrate to maintain osmolarity demonstrates a hyperbolic dependence on [Na^+]. The difference in uptake between NTT4/XT1-chi-expressing cells and control cells at each extracellular [Na^+] was normalized to the subtracted value obtained at 120 mM Na^+. *B,* NTT4/XT1-chi-mediated Pro uptake quantified after a 5-min incubation of transfected HEK293T cells in assay buffer (120 mM NaGluc, pH 8.5) either alone (*control*) or with the addition of 20 μM valinomycin (*val*), 25 mM potassium tartrate (K^+), or both (*val* + K^+) indicates additive inhibition by valinomycin and potassium. Subtracted values were normalized to assay buffer alone. Conditions with significant differences from control are denoted by *single* ($p < 0.05$) or *double asterisks* ($p < 0.01$). *C,* NTT4/XT1-chi-mediated Pro uptake quantified after a 5-min incubation of transfected HEK293T cells in assay buffer (120 mM NaGluc) at pH 5.5, 6.5, 7.2, 8, 8.5, and 9 indicates a strong inhibition by low pH. Subtracted values were normalized to data obtained at pH 8.5. *D,* NTT4/XT1-chi-mediated Pro uptake was quantified after a 5-min incubation of transfected HEK293T cells in assay buffer (120 mM NaGluc) at pH 8.5, 7.2, and 6.5 in the absence or presence of 10 mM ammonium tartrate. Addition of NH_4^+ attenuates uptake in the presence of an outwardly directly proton gradient, but it has no effect in the absence of a proton gradient or the presence of an inwardly directed proton gradient. Subtracted values were normalized to data obtained at pH 8.5 in the absence of NH_4^+. *Double asterisks* indicate that values are statistically different ($p < 0.01$).

proline uptake *versus* the log of unlabeled substrate, leucine inhibits with the highest affinity followed by proline and then glutamine (Fig. 5*B*). The concentration of substrate that inhibits specific NTT4/XT1-chi-mediated proline uptake by 50% (IC_{50}) is 0.28 ± 0.04 mM for leucine, 0.39 ± 0.05 mM for proline, and 1.60 ± 0.16 mM for glutamine (Fig. 5*D*). To further compare the kinetics of proline *versus* glutamine transport, we measured uptake of either [^{3}H]Pro or [^{3}H]Gln, supplemented with 0–10 mM of the corresponding unlabeled amino acid (Fig. 5*C*). Fitting these data with a nonlinear regression using a least squares (ordinary) fit of the Michaelis-Menten model enabled us to calculate the apparent K_m for proline as 0.36 ± 0.02 mM, the apparent K_m for glutamine as 5.2 ± 1.5 mM, the V_{max} for proline as 10.0 ± 0.5 nmol/well/5 min, and the V_{max} for glutamine as 17.6 ± 0.4 nmol/well/5 min (Fig. 5*D*).

Ca^{2+} Ionophore, Ionomycin, Increases Transport Activity of NTT4/XT1 in PC12 Cells—Previous studies have demonstrated that NTT4/XT1 is localized to synaptic vesicles *in vivo*. To test whether the activity of the protein could be coupled to vesicle exocytosis, we expressed NTT4/XT1 in PC12 cells, a rat pheochromocytoma-derived neurosecretory cell line. PC12 cells exhibit many characteristics of neurons, including Ca^{2+}-dependent exocytosis of synaptic like microvesicles. Stable cell lines expressing HA-tagged wild-type NTT4/XT1 were generated, and double label immunofluorescence studies (Fig. 6*A*) indicate that the HA-tagged protein partially co-localizes with synaptobrevin, a protein that localizes to synaptic like microvesicles and large dense core vesicles in PC12 cells (20). The stably expressing cells exhibit a 2.4-fold increase in proline uptake compared with wild-type PC12 cells, suggesting expression of a portion of the recombinant protein on the cell surface (Fig. 6*B*). To induce Ca^{2+}-dependent exocytosis of vesicles without markedly altering the extracellular ionic composition, we used ionomycin, a calcium ionophore (21). In the absence of ionomycin, extracellular Ca^{2+} has no effect on NTT4/XT1-dependent transport, but in the presence of ionomycin addition of 2.2 mM Ca^{2+} to the transport assay buffer increases transport by 28 ± 4% (Fig. 6*C*). To determine whether NTT4/XT1 might also mediate vesicular accumulation of its substrates, we assayed for uptake of proline into vesicles isolated from these same cells. In contrast to a recent report (22) we were unable to detect vesicular proline transport in preparations from the wild-type or stable cells in the presence or absence of ATP (data not shown).

DISCUSSION

Although SLC6A17 (NTT4/XT1) was first identified more than a decade ago, its biochemical function has remained unknown. The predominant localization of heterologously expressed NTT4/XT1 to intracellular membranes has likely impeded its functional characterization. Therefore, we have developed a system to express the recombinant protein at high levels on the plasma membrane in HEK293T cells. This approach has allowed us to directly demonstrate that NTT4/XT1 catalyzes the Na^+-dependent transmembrane transport of neutral amino acids. Given that NTT4/XT1 exhibits observed substrate specificity and apparent affinities similar to those of B^0AT2/SBAT1 (21, 22), we propose that NTT4/XT1 be designated B^0AT3 for the broad (B) specificity for uncharged (0) amino acids. In addition, we show that amino acid uptake by a neurosecretory cell line expressing wild-type B^0AT3 is enhanced in the presence of a calcium ionophore, suggesting that Ca^{2+}-mediated vesicle exocytosis redistributes B^0AT3 to the plasma membrane. This finding demonstrates a

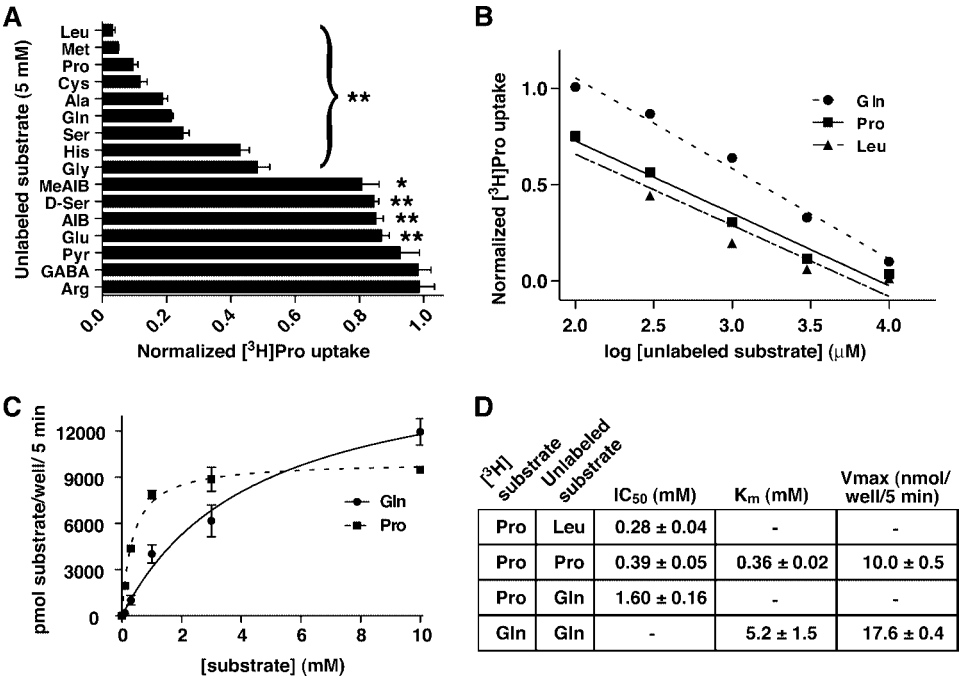

[3H] substrate	Unlabeled substrate	IC_{50} (mM)	K_m (mM)	Vmax (nmol/well/5 min)
Pro	Leu	0.28 ± 0.04	-	-
Pro	Pro	0.39 ± 0.05	0.36 ± 0.02	10.0 ± 0.5
Pro	Gln	1.60 ± 0.16	-	-
Gln	Gln	-	5.2 ± 1.5	17.6 ± 0.4

FIGURE 5. **NTT4/XT1-mediated uptake is differentially inhibited by various amino acids and exhibits substrate-specific kinetic behavior.** *A,* NTT4/XT1-chi-mediated Pro uptake quantified after a 5-min incubation of transfected cells in assay buffer (120 mM NaGluc, pH 8.5) in the absence or presence of 5 mM unlabeled amino acids indicates greatest inhibition by neutral amino acids. Subtracted data were normalized to proline uptake in the absence of unlabeled amino acids. *Single* ($p < 0.05$) or *double asterisks* ($p < 0.01$) indicate significant differences from uptake in the absence of unlabeled substrate. Standard three letter abbreviations are used for amino acids. L-Pyroglutamic acid, α-methylaminoisobutyric acid, α-aminoisobutyric acid, and γ-aminobutyric acid are indicated by *Pyr*, *MeAIB*, *AIB*, and *GABA*, respectively. *B,* measurement of Pro uptake in assay buffer (120 mM NaGluc, pH 8.5) with 0.1 (zero is not shown here) to 10 mM unlabeled Leu, Pro, or Gln demonstrates that Leu and Pro are more effective inhibitors of ^3H uptake than Gln. Data are normalized to [^{3}H]Pro uptake observed in the absence of unlabeled substrate. *C,* analysis of specific NTT4/XT1-chi-mediated uptake of radiolabeled Gln or Pro quantified after a 5-min incubation of transfected cells in assay buffer (120 mM NaGluc, pH 8.5) plus 0–10 mM of the corresponding unlabeled amino acid indicates that both amino acids are transported, but with different Michaelis-Menten kinetics and saturability. Uptake (picomoles of substrate/well/5 min) is plotted as subtracted values for NTT4/XT1-chi-transfected minus control transfected cells and fit with a nonlinear regression. *D,* summary of *B* and *C*. IC_{50} (μM) represents the concentration of unlabeled substrate that inhibits specific NTT4/XT1-chi-mediated [^{3}H]Pro uptake by 50% as calculated from the linear regression in *B*. K_m and V_{max} values are derived from the nonlinear regression of [^{3}H]Pro and [^{3}H]Gln uptake in the presence of increasing concentrations of unlabeled Pro and Gln (*C*). K_m (mM) is the concentration of substrate at which the rate of uptake is half-maximal.

potential mechanism whereby neuronal activity *in vivo* would regulate the plasma membrane localization of B^0AT3 to promote Na^+-dependent amino acid uptake across the plasma membrane.

In addition to the similarity in structure, Na^+ dependence, and substrate specificity, B^0AT3 resembles B^0AT2/SBAT1 in its relative abundance in the nervous system. The primary distinguishing characteristic appears to be the subcellular localization. B^0AT2/SBAT1 is expressed predominantly on the plasma membrane, whereas B^0AT3 is targeted to synaptic vesicles *in vivo* and intracellular membranes when heterologously expressed (16, 17). Our data suggest that this difference is due, in part, to a targeting domain or domains in the cytosolic carboxyl terminus of B^0AT3. It is unknown which sequences within this domain are responsible for the targeting effects. Preliminary mutagenesis studies on the conserved sequence DETRFIL in the carboxyl terminus, which conforms to the dileucine-based consensus motif for adaptor protein binding (23), suggest that this sequence does not have a marked effect on trafficking. More extensive studies will be necessary to determine which sequences within the carboxyl terminus and what other domains of B^0AT3 are involved in proper targeting of the protein to synaptic vesicles.

Differences in coupling mechanisms have been proposed for the transporters in the SLC6 family. For example, the Na^+:substrate stoichiometry varies between 1:1 and 3:1 (4). Although B^0AT3 is clearly Na^+-dependent, only three of the five residues predicted to bind Na_1 based on the LeuT structure are conserved in B^0AT3 (Gly-20, Val-23, and Ser-355), whereas the other two (Ala-351 and Thr-354 in LeuT) are leucine and glycine, respectively, in B^0AT3. Similarly, only two of the four residues that bind Na_2 in LeuT are conserved in B^0AT3 (Asn-27 and Asn-286 are conserved, whereas Ala-22 and Thr-253 are serine and alanine, respectively). Cooperativity is not evident in the Na^+ dependence of B^0AT3-mediated uptake, but this does not exclude the possibility of a stoichiometry other than 1:1. Direct measurement of the current-flux ratio may be needed to determine the stoichiometry. However, given the V_{max} of B^0AT3, transport coupled currents, if present, may be difficult to detect.

Recent work has identified residues that are implicated in binding Cl^- and in conferring the Cl^- dependence of the SLC6 neurotransmitter transporters (14, 15). A proposed model has a Cl^- coordinated by Tyr-121, Ser-336, Asn-368, and Ser-372 of the human SERT. Sequence comparison of other family members reveals that these residues are absolutely conserved in the Cl^--dependent transporters (GAT1–3, BGT1, NET, DAT, GlyT1, GlyT2, CT1, ATB^{0+}, TauT, imino, and PROT), whereas they are not in the structurally related Cl^--independent bacterial proteins LeuT, TnaT, and TyT1. Mutations of these residues in GAT1 and SERT alter the Cl^- dependence of these proteins and mutation of residue 290 in LeuT, which corresponds to Ser-372 in SERT, from glutamate to serine leads to a Cl^- dependence of the transport activity, supporting the model. In each of the Cl^--independent SLC6 transporters (B^0AT1, B^0AT2, and B^0AT3), only one of these four residues corresponding to Cl^--coordinating amino acids is not conserved. In B^0AT1 the residue corresponding to Tyr-121 is a phenylalanine, and in both B^0AT2 and B^0AT3 the residue corresponding to Ser-336 is an alanine. Because the hydroxyl groups of the Tyr-121 and Ser-336 coordinate the Cl^- ion, it

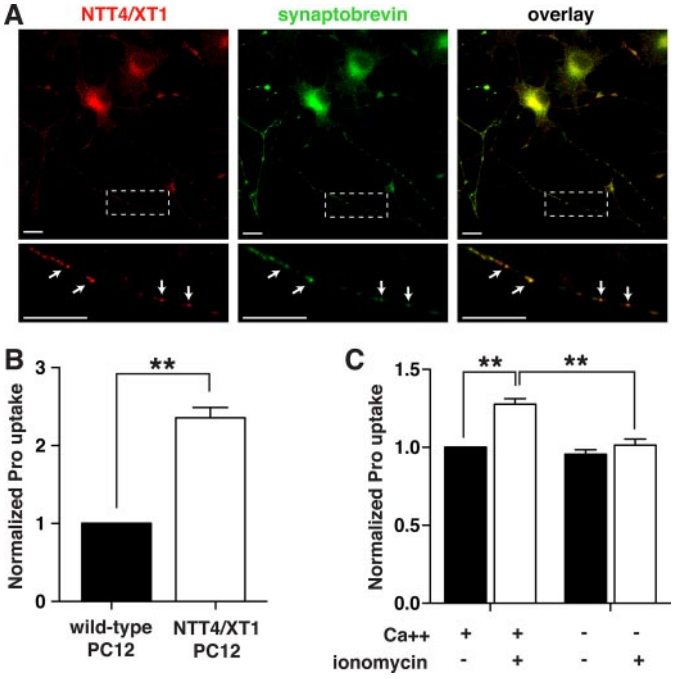

FIGURE 6. **PC12 cells expressing wild-type NTT4/XT1 exhibit Pro uptake activity that is enhanced in the presence of a calcium ionophore.** *A,* differentiated PC12 cells stably expressing HA-tagged wild-type NTT4/XT1 protein were co-immunostained with α-HA (*red*) and α-synaptobrevin (*green*) antibodies. An enlarged view of the demarcated region is shown in the bottom panels. *Scale bars* in both sets of images correspond to 10 μm. *Arrows* denote puncta along a cellular process that exhibit co-localization of NTT4/XT1 and synaptobrevin. *B,* uptake of Pro by wild-type PC12 cells and NTT4/XT1-expressing PC12 cells was quantified after a 5-min incubation in assay buffer (120 mM NaCl, pH 8.5). Normalization to uptake by wild-type PC12 cells shows a 2.4-fold increase in Pro transport by NTT4/XT1-expressing cells. *C,* NTT4/XT1-mediated Pro uptake in PC12 cells was quantified after a 5-min incubation in assay buffer (120 mM NaCl, pH 8.5) in the presence or absence of 2.2 mM $CaCl_2$ either alone (*black*) or with addition of 0.5 μM ionomycin (*white*). Uptake is plotted as subtracted values (NTT4/XT1-expressing PC12 cells minus wild-type PC12 cells) normalized to uptake in the presence of Ca^{2+} alone. *Asterisks* in *B* and *C* denote $p < 0.01$.

is very likely that these specific residues are responsible, in part, for the lack of Cl^- dependence in B^0AT1, B^0AT2, and B^0AT3.

The transport activities of both B^0AT2 and B^0AT3 are remarkably pH-dependent, but the underlying mechanism for this is unclear. A similar robust activation by elevated pH has been demonstrated in a number of other transporters in the SLC6 family, including the mouse GAT4, GlyT1b, and B^0AT1 (18, 19, 24). The reduction in B^0AT3-mediated transport associated with dissipation of the pH gradient by ammonium ions suggests that H^+ antiport may be coupled to proline uptake. However, previous studies with B^0AT2 suggest that the pH sensitivity is not because of the transmembrane pH gradient (9). A more comprehensive analysis of the effect of ΔpH on transport activity of these proteins and/or direct determination of the presence or absence of intracellular pH changes associated with amino acid transport mediated by these proteins will be required to resolve the role of extracellular pH and the transmembrane pH gradient in regulating B^0AT3.

Whereas cell-specific expression patterns, synaptic vesicle localization, and the biochemical characterization of B^0AT3 provide some clues, the physiological role of the protein remains unclear. Its expression in glutamatergic and some GABAergic neurons suggests a substrate for which glutamatergic/GABAergic neurons have a relatively greater need in comparison with other neuronal subtypes. Our studies with PC12 cells and the synaptic vesicle localization of B^0AT3 *in vivo* along with its Na^+ dependence suggest that B^0AT3 function is coupled, in part, to synaptic vesicle fusion with the plasma membrane. This implies a physiological role that is tightly coupled to synaptic transmission.

What is the specific role of B^0AT3? It is tempting to conclude that similar to the Na^+-dependent choline transporter CHT, which localizes to synaptic vesicles in cholinergic neurons, B^0AT3 is mediating uptake of a precursor used in the synthesis of a neurotransmitter (1). If this is the case, then the obvious choice for its physiological substrate is glutamine, which is a metabolic precursor of both glutamate and GABA (25). The concentration of glutamine is 10 times higher than any other amino acid in the cerebrospinal fluid (26). Although it has been suggested that the system A transporters SNAT1 and SNAT2 are involved in glutamine uptake by glutamatergic neurons, recent anatomical and pharmacological studies argue against this (27, 28). Thus B^0AT3 and/or B^0AT2 activity could be supplying glutamine to these neurons.

Given the broad substrate specificity of B^0AT3, a number of other potential roles must be considered. B^0AT3 may contribute to glutamate synthesis by supplying amino acids that provide amine groups for the synthesis of glutamate from α-ketoglutarate. Of note, it has been estimated that nearly one-third of the nitrogen utilized for glutamate synthesis in rat brain is supplied by the branched chain amino acids leucine, isoleucine, and valine (29), all likely substrates of B^0AT3. Alternatively, B^0AT3 might function to remove a neurochemically active substrate from the synapse. For example, proline and glycine, both likely substrates for B^0AT3, have been shown to modulate glutamatergic signaling (30, 31). It is interesting to note that PROT, B^0AT2, B^0AT3, and the brain-specific isoform of the imino transporter are all expressed with relative specificity in the brain and all transport proline with apparent affinities in the submillimolar range. Methionine, another potential physiological substrate for B^0AT3, provides the methyl groups for *S*-adenosylmethionine-dependent methylation reactions and is a precursor of homocysteic acid, which may activate glutamate receptors (32). Finally, given the synaptic vesicle localization of B^0AT3, a role in vesicular transport must also be considered. This is of particular relevance if B^0AT3 transport is coupled to H^+ exchange, as the proton electrochemical gradient generated by the synaptic vesicle vacuolar type H^+-ATPase would drive vesicular accumulation of substrates. However, we have been unable to demonstrate B^0AT3-dependent vesicular uptake.

Regardless of the physiological role of B^0AT3, the similar substrate specificity, ionic dependence, and pH dependence of B^0AT2 and B^0AT3 suggest that they may have some functional redundancy. This may explain, in part, the mild phenotype of the B^0AT2/SBAT1-deficient mice (33), and this suggests that defining the role of these proteins may prove difficult. Furthermore, the synaptic vesicle localization of B^0AT3 suggests that its role may be uniquely relevant during periods of intense neuronal activity.

In characterizing the function of B^0AT3, we have increased our understanding of the mechanisms that underlie amino acid metabolism in neurons. We have demonstrated a direct role for the protein in the transmembrane transport of neutral amino acids, identified a domain involved in targeting the protein to intracellular membranes, and defined its basic biochemical characteristics. Coupling the transport characteristics of B^0AT3 with a comparison of its structure to other members of the SLC6 family of transporters may also reveal important insights into the mechanistic differences among these structurally related, but functionally divergent, proteins.

Acknowledgments—We greatly appreciate the gift of the dynamin dominant negative plasmid from Randy Blakely (Vanderbilt University, Nashville, TN). We acknowledge Craig Garner and the members of the Garner laboratory for assistance with the microscopy and Merritt Maduke and members of the Reimer laboratory for critical review of the manuscript.

REFERENCES

1. Ferguson, S. M., Savchenko, V., Apparsundaram, S., Zwick, M., Wright, J., Heilman, C. J., Yi, H., Levey, A. I., and Blakely, R. D. (2003) *J. Neurosci.* **23,** 9697–9709
2. Edwards, R. H. (2007) *Neuron* **55,** 835–858
3. McKenna, M. C. (2007) *J. Neurosci. Res.* **85,** 3347–3358
4. Chen, N. H., Reith, M. E., and Quick, M. W. (2004) *Pfluegers Arch.* **447,** 519–531
5. Broer, S. (2006) *Neurochem. Int.* **48,** 559–567
6. el Mestikawy, S., Giros, B., Pohl, M., Hamon, M., Kingsmore, S. F., Seldin, M. F., and Caron, M. G. (1994) *J. Neurochem.* **62,** 445–455
7. Liu, Q. R., Mandiyan, S., Lopez-Corcuera, B., Nelson, H., and Nelson, N. (1993) *FEBS Lett.* **315,** 114–118
8. Takanaga, H., Mackenzie, B., Peng, J. B., and Hediger, M. A. (2005) *Biochem. Biophys. Res. Commun.* **337,** 892–900
9. Broer, A., Tietze, N., Kowalczuk, S., Chubb, S., Munzinger, M., Bak, L. K., and Broer, S. (2006) *Biochem. J.* **393,** 421–430
10. Sambrook, J., and Russell, D. (2001) *Molecular Cloning: A Laboratory Manual*, 3rd Ed., Cold Spring Harbor Laboratory Press, Cold Spring Harbor, NY
11. Zhang, J., Ferguson, S. S., Barak, L. S., Menard, L., and Caron, M. G. (1996) *J. Biol. Chem.* **271,** 18302–18305
12. Wreden, C. C., Wlizla, M., and Reimer, R. J. (2005) *J. Biol. Chem.* **280,** 1408–1416
13. Yamashita, A., Singh, S. K., Kawate, T., Jin, Y., and Gouaux, E. (2005) *Nature* **437,** 215–223
14. Forrest, L. R., Tavoulari, S., Zhang, Y. W., Rudnick, G., and Honig, B. (2007) *Proc. Natl. Acad. Sci. U. S. A.* **104,** 12761–12766
15. Zomot, E., Bendahan, A., Quick, M., Zhao, Y., Javitch, J. A., and Kanner, B. I. (2007) *Nature* **449,** 726–730
16. Masson, J., Riad, M., Chaudhry, F., Darmon, M., Aidouni, Z., Conrath, M., Giros, B., Hamon, M., Storm-Mathisen, J., Descarries, L., and El Mestikawy, S. (1999) *Eur. J. Neurosci.* **11,** 1349–1361
17. Farmer, M. K., Robbins, M. J., Medhurst, A. D., Campbell, D. A., Ellington, K., Duckworth, M., Brown, A. M., Middlemiss, D. N., Price, G. W., and Pangalos, M. N. (2000) *Genomics* **70,** 241–252
18. Aubrey, K. R., Mitrovic, A. D., and Vandenberg, R. J. (2000) *Mol. Pharmacol.* **58,** 129–135
19. Grossman, T. R., and Nelson, N. (2002) *FEBS Lett.* **527,** 125–132
20. Papini, E., Rossetto, O., and Cutler, D. F. (1995) *J. Biol. Chem.* **270,** 1332–1336
21. Pozzan, T., Gatti, G., Dozio, N., Vicentini, L. M., and Meldolesi, J. (1984) *J. Cell Biol.* **99,** 628–638
22. Parra, L. A., Baust, T. B., El Mestikawy, S., Quiroz, M., Hoffman, B., Haflett, J. M., Yao, J. K., and Torres, G. E. (2008) *Mol. Pharmacol.* **74,** 1521–1532
23. Bonifacino, J. S., and Traub, L. M. (2003) *Annu. Rev. Biochem.* **72,** 395–447
24. Broer, A., Klingel, K., Kowalczuk, S., Rasko, J. E., Cavanaugh, J., and Broer, S. (2004) *J. Biol. Chem.* **279,** 24467–24476
25. Albrecht, J., Sonnewald, U., Waagepetersen, H. S., and Schousboe, A. (2007) *Front. Biosci.* **12,** 332–343
26. McGale, E. H., Pye, I. F., Stonier, C., Hutchinson, E. C., and Aber, G. M. (1977) *J. Neurochem.* **29,** 291–297
27. Conti, F., and Melone, M. (2006) *Neurochem. Int.* **48,** 459–464
28. Kam, K., and Nicoll, R. (2007) *J. Neurosci.* **27,** 9192–9200
29. Garcia-Espinosa, M. A., Wallin, R., Hutson, S. M., and Sweatt, A. J. (2007) *J. Neurochem.* **100,** 1458–1468
30. Sur, C., and Kinney, G. G. (2007) *Curr. Drug Targets* **8,** 643–649
31. Cohen, S. M., and Nadler, J. V. (1997) *Brain Res.* **761,** 271–282
32. Thompson, G. A., and Kilpatrick, I. C. (1996) *Pharmacol. Ther.* **72,** 25–36
33. Drgonova, J., Liu, Q. R., Hall, F. S., Krieger, R. M., and Uhl, G. R. (2007) *Brain Res.* **1183,** 10–20